Water Research 221 (2022) 118721

Contents lists available at ScienceDirect

Water Research

journal homepage: www.elsevier.com/locate/watres

Reservoir water quality deterioration due to deforestation emphasizes the indirect effects of global change

Xiangzhen Kong [a,b,*], Salman Ghaffar [c,d], Maria Determann [b], Kurt Friese [b], Seifeddine Jomaa [c], Chenxi Mi [b], Tom Shatwell [b], Karsten Rinke [b], Michael Rode [c,e]

[a] State Key Laboratory of Lake Science and Environment, Nanjing Institute of Geography and Limnology, Chinese Academy of Sciences, Nanjing, China
[b] Department of Lake Research, Helmholtz Centre for Environmental Research (UFZ), Magdeburg, Germany
[c] Department of Aquatic Ecosystem Analysis and Management, Helmholtz Centre for Environmental Research (UFZ), Magdeburg, Germany
[d] Leichtweiß-Institute for Hydraulic Engineering and Water Resources, Technische Universität Braunschweig, Braunschweig, Germany
[e] Institute of Environmental Science and Geography, University of Potsdam, Potsdam-Golm, Germany

ARTICLE INFO

Keywords:
Deforestation
Climate change
Temperate regions
Reservoir
Eutrophication
Process-based modeling

ABSTRACT

Deforestation is currently a widespread phenomenon and a growing environmental concern in the era of rapid climate change. In temperate regions, it is challenging to quantify the impacts of deforestation on the catchment dynamics and downstream aquatic ecosystems such as reservoirs and disentangle these from direct climate change impacts, let alone project future changes to inform management. Here, we tackled this issue by investigating a unique catchment-reservoir system with two reservoirs in distinct trophic states (meso- and eutrophic), both of which drain into the largest drinking water reservoir in Germany. Due to the prolonged droughts in 2015–2018, the catchment of the mesotrophic reservoir lost an unprecedented area of forest (exponential increase since 2015 and ca. 17.1% loss in 2020 alone). We coupled catchment nutrient exports (HYPE) and reservoir ecosystem dynamics (GOTM-WET) models using a process-based modeling approach. The coupled model was validated with datasets spanning periods of rapid deforestation, which makes our future projections highly robust. Results show that in a short-term time scale (by 2035), increasing nutrient flux from the catchment due to vast deforestation (80% loss) can turn the mesotrophic reservoir into a eutrophic state as its counterpart. Our results emphasize the more prominent impacts of deforestation than the direct impact of climate warming in impairment of water quality and ecological services to downstream aquatic ecosystems. Therefore, we propose to evaluate the impact of climate change on temperate reservoirs by incorporating a time scale-dependent context, highlighting the indirect impact of deforestation in the short-term scale. In the long-term scale (e.g. to 2100), a guiding hypothesis for future research may be that indirect effects (e.g., as mediated by catchment dynamics) are as important as the direct effects of climate warming on aquatic ecosystems.

1. Introduction

Global deforestation is proceeding at unprecedented rates, driven by increasing events of wildfires, droughts, heatwaves, pests and pathogens (Mottl et al., 2021; Overpeck and Breshears, 2021). Forest has been well-acknowledged as high priority habitats as they store high biodiversity and provide key ecosystem services (Mori et al., 2017). Among them, the positive feedbacks between forests and the water cycle are multifaceted and not only refer to water quantity dynamics but also to water quality, e.g., by buffering of nutrients, reducing erosion, or enhancing in-stream removal processing of nutrients, thereby serving as a major management target for catchment-centered water quality restoration (Sweeney et al., 2004). In contrast, deforestation leads to loss of key ecosystem functions and induces legacy effects on the catchment hydrosphere by changing runoff patterns or intensifying nutrient loading from these catchments (Woodward et al., 2014). Thus far, large-scale deforestation has been recognized as a key driver for the changes in the biogeochemical cycling at local and global scales (Lawrence and Vandecar, 2015).

Deforestation in temperate regions, particularly in central European

* Corresponding author at: State Key Laboratory of Lake Science and Environment, Nanjing Institute of Geography and Limnology, Chinese Academy of Sciences, Nanjing, China.
E-mail address: xzkong@niglas.ac.cn (X. Kong).

https://doi.org/10.1016/j.watres.2022.118721
Received 31 January 2022; Received in revised form 16 May 2022; Accepted 5 June 2022
Available online 7 June 2022

uplands, has been relatively understudied compared to tropical areas. In many tropical, densely forested areas (e.g., the Amazon), deforestation effects are predominantly addressed regarding catchment exports of particulate substances (Bormann et al., 1974), nutrient cycling (Downing et al., 1999), and system resilience (Zemp et al., 2017). However, despite the ongoing widespread deforestation in central Europe, only a few studies in Poland (Boczoń et al., 2018), the Czech Republic (Schmidt et al., 2021) and Germany (Jung et al., 2021) were recently performed, which all pointed to a change in dissolved mass export from the catchment, but with contradictory trends, varying magnitudes and temporal patterns. Our predictive ability to assess the impact of deforestation in temperate region therefore remains limited. Climate change and increasing deforestation (Overpeck and Breshears, 2021), as well as the significant difference in hydrogeological processes between temperate and tropical systems (Domis et al., 2013), jointly call for more in-depth explorations of the deforestation effects on catchment dynamics in the central European temperate regions.

Furthermore, the consequences of deforestation for the downstream waterbodies such as reservoirs have been rarely addressed in central Europe. Reservoirs are highly valuable artificial infrastructures providing various ecological services to human, including drinking water resources, nutrient removal to downstream, and flood protection (Rinke et al., 2013). In particular, small reservoirs constitute most existing reservoirs and are disproportionately important for biogeochemical processes (Harrison et al., 2009). They usually have a relatively short water residence time and are highly sensitive to both climate change and anthropogenic perturbations (Adrian et al., 2009). Nevertheless, except for a few cases that focused on specific water chemistry proxies (Kopáček et al., 2017, 2019), the impact of deforestation on the ecosystem dynamics in downstream reservoirs has been largely overlooked despite its vast management concern.

It is challenging to attribute the direct and indirect impacts on reservoir ecology to external forces. Direct effects from climate change on water bodies have been well-acknowledged (Woolway et al., 2020), whereas joint effects from indirect effects in the catchment via land-use change, including deforestation, remain largely unquantified. Disentangling the effects is valuable because only a comprehensive integration of direct and indirect impacts can thoroughly inform management, e.g., by prioritizing alternative mitigation measures either targeting catchment or reservoir focused management response. A feasible method to address this challenge is to use process-based models driven by different external forcing scenarios to project ecosystem dynamics in the future. It is pivotal to bring the following five environmental compartments into one coherent chain of processing: climatic physical drivers, catchment hydrology, biogeochemical processing in the catchment, lake physics and aquatic ecology. However, such efforts are rare and existing approaches usually simplified either the catchment or the lake/reservoir compartments depending on their research emphases (Barbosa et al., 2021; Couture et al., 2014; Nielsen et al., 2021), thereby missing key mechanisms related to deforestation and its impact on lake/reservoir ecosystem dynamics. From the perspective of environmental modeling, integrating the five modeling modules is challenging yet highly valuable.

In addition, future projections of lakes responding to climate change have focused predominantly on physical properties (such as temperature and stratification; e.g., Woolway et al. (2020)), and less frequently on water quality or ecology (Jane et al., 2021; Kraemer et al., 2021). In addition, these projections fundamentally cannot be validated. Reference systems are therefore extremely valuable for the validation of these projections. However, such opportunities are rare because most systems are substantially different in morphology, water chemistry and ecological features, which hampers direct comparison. Availability of monitoring data is another key determinant for such a comparative approach. Grab sampling is usually limited to offering a comprehensive understanding of a complex interacting catchment-reservoir system. Instead, high-frequency monitoring approach representing the catchment and reservoir heterogeneities are recommended (Rode et al., 2016).

In this study, we utilize a unique catchment-reservoir system in central Germany with two predams with similar morphological features but distinct trophic states (meso- and eutrophic). The difference in trophic status is mainly driven by land use in the catchments with either forest- or agriculture dominance. These two systems have been intensively monitored at both catchment outlets and reservoirs since 2011, allowing for adequate modeling exploration. The hypotheses are: 1) large-scale deforestation in temperate catchments of central European uplands can lead to increased nutrient fluxes to the downstream via an increase in both discharge and concentration; 2) jointly with climate warming, the changes in catchment nutrient exports can subsequently turn the downstream lake/reservoir from meso- into eutrophic state and deteriorating the water quality. To address these hypotheses, we established a coupled catchment (HYPE) and reservoir (GOTM-WET) model, which was used to project reservoir water quality by 2035 under various climate change and deforestation scenarios. We elaborated to disentangle the relative importance of climate change and deforestation, and provide new insights for combating future climate change effects and safeguarding the water resources.

2. Materials and methods

2.1. Study sites

The Rappbode and Hassel predams are located in the eastern Harz Mountains in central Germany (Fig. 1 and Table 1). The two predams drain directly into the main Rappbode Reservoir (two-thirds of total inflow), which is the largest drinking water reservoir in Germany for about one million residents and providing additional services such as flood protection and electricity production (Rinke et al., 2013). The two predams were built to reduce sediment and nutrient load to the main reservoir. They are operated in continuous overflow on the spillway while the bottom outlets are normally closed. They share similar morphological properties and catchment size (Friese et al., 2014). However, whereas the Rappbode catchment is predominantly forest without agricultural use, the Hassel catchment consists of roughly equal areas of forest, grassland and agriculture. This could explain the distinct trophic states in Rappbode (mesotrophic) and Hassel (eutrophic) predams (Table 1). In addition, the Rappbode catchment underwent deforestation of ca. 17.1% from 2015 to 2020 (Figs. 1 and S1). Since 1999, all wastewater from the settlements in the two catchments are collected and treated outside the catchment. Sampling stations were deployed at the inflow (YRZ for Rappbode, YHZ-Q and YHZ-WQ for Hassel), the deepest points in the reservoir (YR3 and YH3 for Rappbode and Hassel, respectively), and the reservoir outflow closest to the dam (YR1 and YH1 for Rappbode and Hassel, respectively)(Fig. 1). All monitoring activities are part of the TERENO lowland observatory networks across Germany (www.tereno.net).

2.2. Data collection for modeling

Meteorological data to drive the catchment and lake model were collected from the German meteorology service (DWD) via the package 'rdwd' (Boessenkool, 2019) in R (R Core Team, 2021), at three climate stations and seven precipitation gage stations from Jan. 1st, 2010 to Dec. 31st, 2019 (Figs. S2 and S3). Collected variables included air temperature (°C), air pressure (hPa), relative humidity (%), mean wind speed (m s^{-1}) and precipitation (mm) at hourly interval, and shortwave radiation (J cm^{-2}) for every 10 min (aggregated to hourly).

Daily discharge at the gage stations of both inflows (YRZ and YHZ-Q) from 2010 to 2019 were provided by the local environmental authority "Landesbetrieb für Hochwasserschutz und Wasserwirtschaft (LHW)". The gage station for the Hassel catchment (YHZ-Q) is located 2 km upstream of the inlet so that ~35% of the catchment is not covered, which is corrected by the catchment modeling (see below). High frequency (10

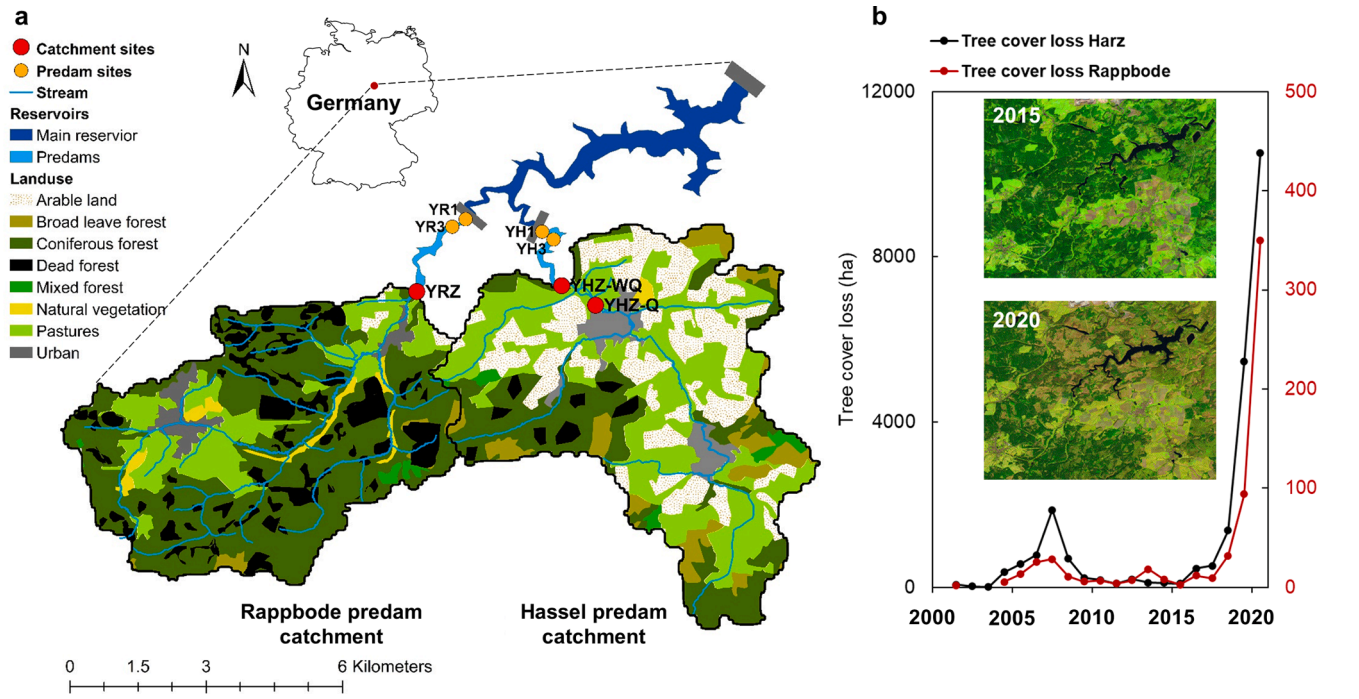

Fig. 1. (a) Land use distributions in the catchments of Rappbode (mesotrophic) and Hassel (eutrophic) predams in the Harz Mountain, central Germany. Locations of the seven water quality monitoring sites are provided, including catchment outlets (YRZ and YHZ-Q/WQ) and inside the predams (YR1 and YR3, YH1 and YH3). For Hassel catchment, gaging station (YHZ-Q) is 2 km upstream of the water quality station (YHZ-WQ). The areas of dead forest in the catchments are determined by remote sensing imagery from Sentinel-2 (2020). Land use surrounds the predams and the main reservoirs can be found in Friese et al. (2014). (b) Deforestation (provided as area of tree cover loss) in the whole Harz Mountain and the Rappbode catchment from 2001 to 2020, with noteworthy exponential tree cover loss since 2015. Inner panels are remote sensing imageries from Sentinel-2 in both 2015 and 2020.

Table 1
Summary overview of the two predam reservoirs (Rappbode and Hassel) and their corresponding catchments (based on Rinke et al. (2013) and Friese et al. (2014)). TN, TP and Chl-a concentrations in the reservoirs are the column-weighted average values during the monitoring period (2011–2015) at sites YR3 and YH3 (Fig. 1a), and the TSI is calculated based on Carlson (1977) (TSI<30: oligotrophic; 30<TSI<50: mesotrophic; TSI>50: eutrophic; see SI text for more details).

Characteristic	Unit	Rappbode	Hassel
Catchment			
Catchment area	km^2	42.9	40.5
Average altitude	m	533	504
Annual discharge	mm	374	249
Annual precipitation	mm	854	758
Forest	%	78	36
Pastures	%	15	29
Arable land	%	1	26
Urban	%	3	5
Others	%	3	4
Reservoir			
Surface area	km^2	0.243	0.260
Storage capacity	Mm^3	1.66	1.44
Max. water depth	m	16	14
Mean water depth	m	5.3	5.0
Residence time	day	51.7	65.2
Total Nitrogen (TN)	mg L^{-1}	0.98 (±0.41)	2.97 (±1.36)
Total Phosphorus (TP)	mg L^{-1}	0.025 (±0.006)	0.043 (±0.013)
Chl-a	μg L^{-1}	7.52 (±12.92)	13.51 (±24.43)
Trophic state index (TSI)	-	45.1 (±3.5) (Mesotrophic)	57.3 (±2.9) (Eutrophic)

min interval) continuous measurements on concentrations of NO_3—N in both inflows were performed by optical probe (ProPS, TRIOS, Germany) measuring light extinction in the UV spectrum (190–360 nm). Grubbs' test (Grubbs, 1950) was used to eliminate outliers for pre-processing. The data were aggregated to a daily basis to facilitate the comparison with HYPE outcomes. In addition, water samples from the streams (YRZ and YHZ-WQ) were collected on a biweekly interval for wet chemical analysis in the laboratory, including total nitrogen (TN), Nitrate-N (NO_3—N), Ammonium (NH_4—N), particulate nitrogen (PN), total phosphorus (TP), dissolved phosphorus (DP), soluble reactive phosphorus (SRP), silicon (Si), and particulate organic carbon (POC). Particulate phosphorus (PP) was calculated as the difference between TP and DP. From 2011 to 2015, vertical profiles of temperature, dissolved oxygen, and chlorophyll-a fluorescence were measured with a multiparameter probe (CTD90, Sea and Sun Technology GmbH, Germany), while the phytoplankton composition in terms of specific chlorophyll-fluorescence from diatoms, green algae, cryptophytes, and cyanophytes (Beutler et al., 2002) was determined with another multi-channel fluorescence probe (Fluoroprobe, bbe moldaenke GmbH, Germany) at the deepest point in the two predams (YR3 and YH3; Fig. 1). Water samples were collected at six depths (2, 5, 8, 10, 12, 15 m (Rappbode)/13 m (Hassel)) for wet chemical analysis in the laboratory on the same chemical variables as those in the streams. In addition, surface water samples (0.5 m) were collected in front of the dam (YR1 and YH1; Fig. 1) on a biweekly interval from 2011 to 2019 for chemical analysis as explained above. Volume-weighted concentrations were calculated for the whole water column during mixing, and separately for the epilimnion and hypolimnion during the stratified period (Fig. S4). The lab methods and data handlings were described by Friese et al. (2014) in more detail.

2.3. Model description and set up

2.3.1. Catchment model

The HYdrological Predictions for the Environment (HYPE) model is a semi-distributed process-based hydrological and water quality model

with the capability of simulating streamflow and nutrient export, and assessing the impact of land-use change on nutrient yields (Lindström et al., 2010). A more recent version (HYPE 4.3.0), which was used for this study, has been specifically adapted to forest processes (Pers et al., 2016). The impact of different land use types on hydrological and nutrient cycling is reflected by model parameters, e.g. the potential evaporation (*cevp*) and denitrification (*Denitr*) are land use dependent (Table S1). The HYPE model simulated from 2010 to 2019 for discharge, NO_3—N and TP concentration. The model was calibrated (2011–2014) and validated (2015–2019) separately, and simulation in 2010 was kept as the 'spin-up' period. For Hassel, discharge and NO_3—N were calibrated at the upstream gage station (YHZ-Q), and TP was calibrated at the downstream station (YHZ-WQ). Input data regarding general agriculture practices, primary and sowings crops were taken from a previous study (Ghaffar et al., 2021). DiffeRential Evolution Adaptive Metropolis tool (DREAM) was applied for calibration and uncertainty analysis. Due to high computation demands, a two-year period (2013–2014) with large variations in discharge was selected as hydrologically critical years. Parameter and total uncertainty related to parameters variations and model structure were evaluated by 10,000 Markov Chain Monte Carlo simulations, and the 95% confidence interval band was considered as the uncertainty range (Ghaffar et al., 2021). A detailed explanation of the DREAM tool could be found in Vrugt et al. (2008). Sensitive parameters for discharge, NO_3—N and TP were identified before (Ghaffar et al., 2021) and the optimized values for this study were provided in Table S1. Performance of the HYPE model to simulate discharge, NO_3—N and TP concentrations was evaluated by both Nash-Sutcliffe Efficiency (*NSE* and log-based *NSE*) and percentage bias (*PBIAS*) (Ullrich and Volk, 2010) (see SI text).

2.3.2. Reservoir ecosystem model

The 1D General Ocean Turbulence Model (GOTM) and the lake ecosystem model Water Ecosystem Tool (WET) (Schnedler-Meyer et al., 2022) was utilized to simulate the ecosystem dynamics in the reservoirs. GOTM-WET simulates the key ecosystem dynamics with a strong vertical heterogeneity, and can be linked to the HYPE model to evaluate the impact of catchments dynamics on the reservoirs. The ecological module is based on the PCLake model with a fully closed biogeochemical cycling (carbon, nitrogen, phosphorus) and a typical foodweb structure of temperate lake/reservoir ecosystems (Hu et al., 2016; Janse, 2005). GOTM-WET was calibrated and validated against a five-year monitoring dataset (2011–2015, in YR3 and YH3) preceded by a one-year spin-up period (2010). The model was additionally validated (second validation) by another dataset at surface water from 2011 to 2019 (YR1 and YH1). Auto-calibration python-based program PARSAC for numerical model simulation (Bolding and Bruggeman, 2020) was applied to perform a global optimization of a subset of model parameters selected by sensitivity analysis (Andersen et al., 2021; Janse et al., 2010; Nielsen et al., 2014). This program applies the differential evolution method (Storn and Price, 1997), which searches for the optimal model parameter set within parameter-specific predefined ranges for a maximum likelihood multi-objective function. Auto-calibration is implemented in a bottom-up approach, including seven steps with the parameters and state variables specifically selected in each step (Andersen et al., 2020). The auto-calibration ends when the model error could no longer be further reduced (see Table S2). Evaluation of the GOTM-WET model is based on the correlation coefficient (*R*), root mean square error (*RMSE*) and percentage of bias (*PBIAS*) (Bennett et al., 2013). Besides, trophic state index (*TSI*) was calculated based on GOTM-WET outputs as a synthetic ecosystem indicator for the reservoir (see SI text).

2.4. Scenario design for future projections

We design a scenario analysis to evaluate the impact of climate change and deforestation on catchment dynamics and ultimately on water quality and trophic states in the reservoirs by 2035. Hourly climate projections for all variables were taken from five Global Climate Models (GCMs) (HadGEM2-ES, IPSL-CM5A-LR, MIROC-ESM-CHEM, GFDL-ESM2M and NorESM1-M) provided by the Inter-Sectoral Impact Model Inter-comparison Project (ISI-MIP) (Warszawski et al., 2014). Scenarios include future climate change projections (2021–2035) of 'piControl' (without anthropogenic climate change) and three Representative Concentration Pathway (RCPs 2.6, 6.0 and 8.5). The data were further interpolated by an external drift kriging method to a 5 km grid over the study area (Fig. S5). Quantile mapping was used for bias correction of RCP inputs (Déqué et al., 2007). In addition, three deforestation scenarios (0, 50 and 80% deforestation) were applied to the Rappbode catchment. For both 50 and 80% deforestation, soil-land classes previously defined as spruce forest (coniferous trees) in the HYPE model were changed to natural grassland cover as a typical natural process after deforestation.

2.5. Statistical analysis

All statistical analyses were performed in R Core Team (2021). The analyses were based on the annually-averaged simulated values during the projection period (2021–2035). Effects of climate change were assessed by comparing model outputs from each RCP scenario in the period 2021–2035 with a historical baseline period of 2011–2018, thereby as a factor with four levels (historical, RCPs 2.6, 6.0, and 8.5). For catchments, the historical baseline was determined by field data in the catchment outlets. For reservoirs, it was determined by simulated data of the reservoir model driven by catchment inputs and climate projection 'piControl'. The effect of deforestation was assessed by comparing modelled variables in the future period with each deforestation as a factor with three levels (0, 50 and 80% loss). Kruskal-Wallis (KW) test (R function 'kruskal.test') was used to test the differences among different projection scenarios. If significant differences were tested, pairwise Wilcoxon test (R function 'pairwise.wilcox.test') was utilized to distinguish the specific different groups. Besides, Wilcoxon test was used to test if the variable was different among the two reservoirs (R function 'wilcox.test'). For temporal trends in time series data, Mann-Kendall (MK) test was utilized (R function 'MannKendall' in package 'Kendall' (McLeod, 2005)).

In addition, multilevel models were used to examine the relative importance (quantified by the percentage of variance explained) of climate change and deforestation and their interactions (as fixed effects) on the future projections of various hydro-ecological variables. Climate change and deforestation scenarios were nested, and different GCMs were provided as replicates. Time was considered as the random effect in the model. The model also estimated the contribution of residuals as the variance not explained by any factor. All variables were naturally log-transformed prior to the analysis to improve the normality. The multilevel models were developed using R packages 'lme4' and 'variancePartition' (Bates et al., 2014; Hoffman and Schadt, 2016).

3. Results

3.1. Catchment model calibration and validation

The HYPE model showed good performance for discharge at both stations during calibration and validation periods (Fig. 2 and Table S3). Seasonal dynamics were well captured including flow conditions, flood events and base flow. The highest *NSE* value (0.81) was observed at Rappbode during validation and lowest *NSE* value (0.74) was at Hassel catchment during calibration. *PBIAS* was below 20% for calibration and validation at both stations and was lower at Rappbode than Hassel.

NO_3—N loading was predicted reasonably well. For calibration, the model performed better in Rappbode than Hassel with *NSE* of 0.54 and 0.36, respectively (*logNSE* provides similar outcomes). During the validation period, the model also showed good performance with *NSE* of 0.71 in Rappbode and 0.49 in Hassel. *PBIAS* values were below 10% for

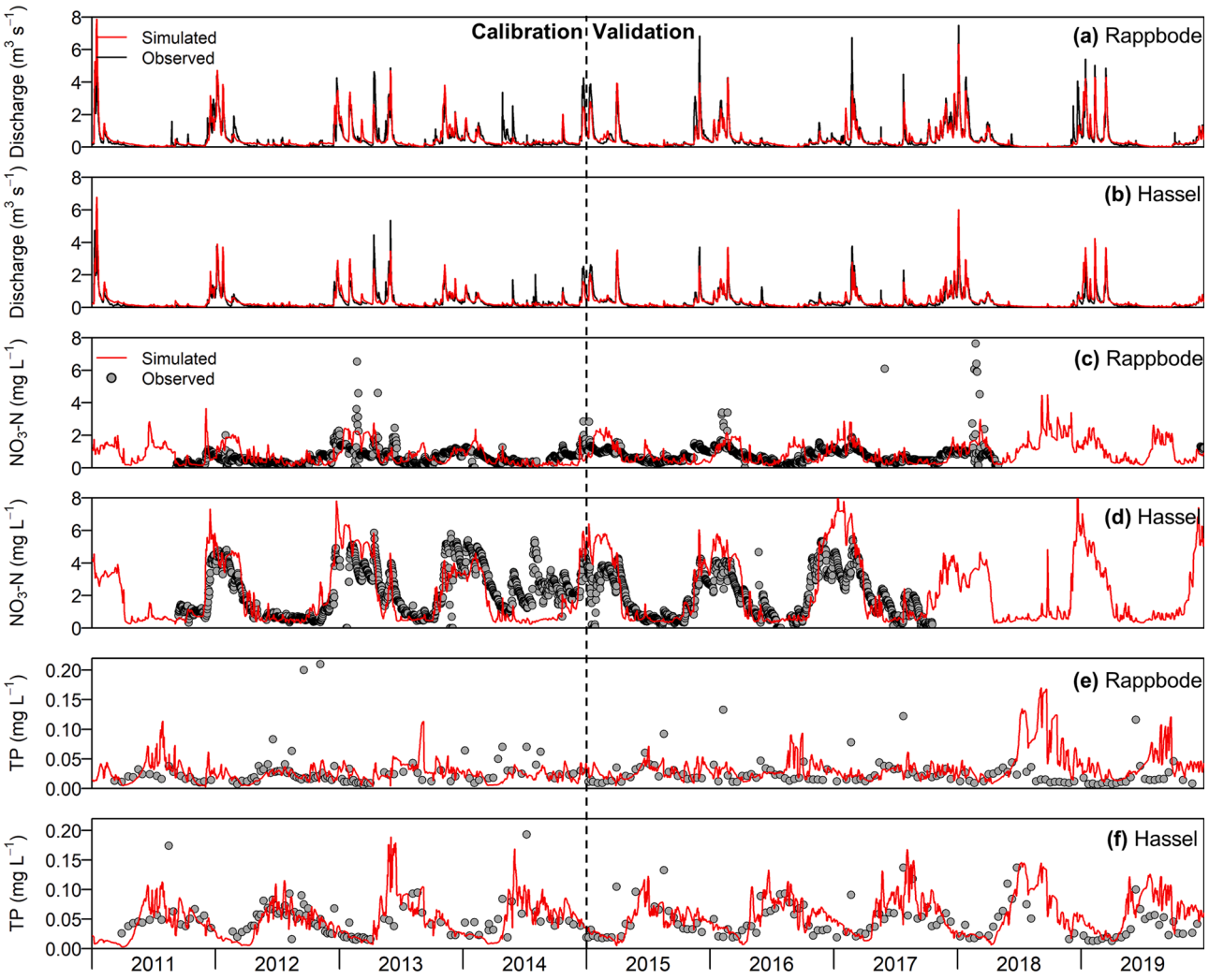

Fig. 2. Performance of the catchment model (HYPE). Simulated and observed discharge (Q), NO_3—N and total phosphorus (TP) concentrations in Rappbode and Hassel catchments are compared during calibration (2011–2014) and validation (2015–2019). Q and NO_3—N concentration are measured at daily intervals, while TP concentrations are measured at biweekly interval in the laboratory. Note that discharge gage and water quality are measured in the same site in Rappbode catchment, but are separated at two stations in Hassel catchment, i.e., Hassel-Q and Hassel-WQ, respectively, (see Fig. 1 for more detail).

calibration and ~20% for validation. NO_3—N concentration shows a typical seasonal cycle with lower concentrations in late summer and high concentration in winter. These patterns were more pronounced in Hassel than in Rappbode and the model could remarkably reproduce these catchment-specific features.

The model showed reasonable performance for TP loading, with *NSE* between 0.12 and 0.45 in both catchments during both calibration and validation periods. *PBIAS* values for both catchments were observed within the satisfactory range (-22% to 21%) except at Hassel during the calibration (40.2%), which was attributed to several simulated summer peaks against lower observed values. Several hydrological events were not captured by the model due to strong areal rainfall variation, which was likely not accurately measured by the limited number of precipitation stations. Consequently, log*NSE* values were better than the original *NSE* values. Nevertheless, the model satisfactorily captured the low flow seasonal TP concentration amplitudes with winter lows and summer highs in both catchments, and the more pronounced seasonality of TP in Hassel than in Rappbode.

The model evaluation for NO_3—N and TP concentrations also reflects good performance in both catchments, with small differences between simulated and observed concentration and *PBIAS* ranged -18.31–17.03% for NO_3—N and -7.34–17.25% for TP (Table S3). Nevertheless, we consider the loads more important than concentrations for the impact on the trophic state of the predams, and evaluation based on concentration using *NSE* and *PBIAS* can be inadequate when the observed values are low and the discrepancy is close to detection limit.

The uncertainty analysis (Fig. S6) shows small parameter uncertainty bands of discharge NO_3—N and TP, indicating the low uncertainty related to parameter optimization. In contrast, total uncertainty shows a much larger range, suggesting higher uncertainty caused by model structural uncertainties. Similar patterns were observed for NO_3—N and TP at both catchments. More than 90% of the observed data for discharge, NO_3—N and TP lies in the total uncertainty bands. Compared to NO_3—N, higher uncertainties were observed for TP due to less observed data for calibration, which can be improved by increasing availability of high frequency data. Taken together, uncertainty associated with HYPE model is acceptable and equifinality of parameterization is unlikely.

3.2. Projections of catchment dynamics

At annually-averaged scale, the model predicts that discharge in Rappbode catchment slightly increases by up to 10.2% (Fig. 3, Table 2) due to climate changes and deforestation (KW test, $p < 0.01$), and the change is significant at RCP6.0 or 8.5, and 50 or 80% deforestation (pairwise Wilcoxon test, $p < 0.05$). Multilevel models show that over

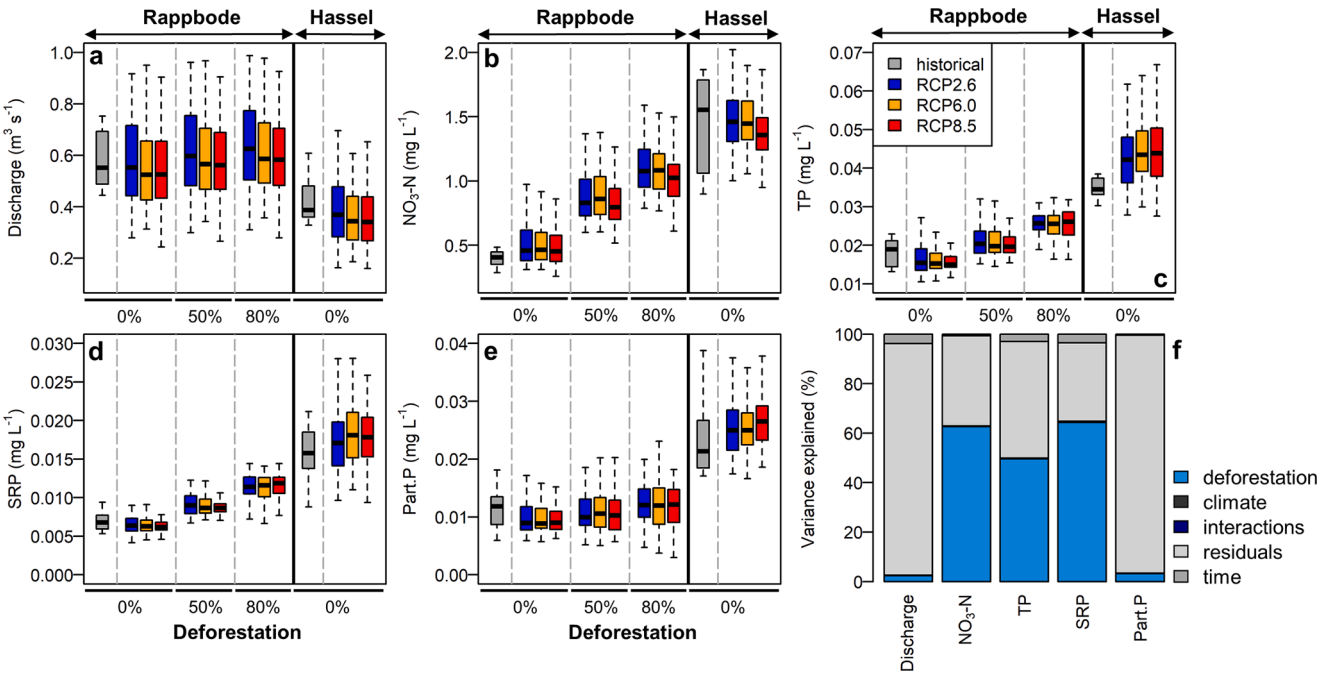

Fig. 3. Projections of catchment dynamics by HYPE. (a-e) Projections for different water quality variables in both Rappbode and Hassel catchments at an annually-averaged scale. The projections include the scenarios of four climate projections (historical and RCPs 2.6, 6.0 and 8.5) and three deforestation rates (0, 50 and 80%). 'Historical' scenario is the measured data from 2011 to 2018 before the deforestation in the catchment, and the other scenarios are from 2021 to 2035. For Hassel, only 0% deforestation is projected serving as a reference state. See Fig. S7 for the time series of these data at a daily scale. (f) Relative contributions of different factors in explaining the variance of various variables projected in the Rappbode catchment, determined by multilevel analysis on the model projections. Note that 'interactions' denote the interactions between deforestation and climate change.

Table 2

Statistical analyses of the model projections for catchment and reservoir ecosystem dynamics in the annually-average scale from 2021 to 2035. Kruskal-Wallis rank sum test shows if there are significant differences between the multiple groups of climate change and deforestation rates, and pairwise Wilcoxon test further distinguishes the difference between paired groups (only deforestation groups are provided). Relative changes show the percentage changes in the annually-average scale under deforestation of 50% and 80% compared to 0%. Note: * $p < 0.05$, ** $p < 0.01$, *** $p < 0.001$. [a] no value due to insignificant change ($p > 0.05$).

Variables	**Kruskal-Wallis rank sum test**				**Pairwise Wilcoxon test (*p*-value)** under deforestation		**Relative changes** under deforestation	
	Climate change (historical, RCPs2.6, 6.0, 8.5)		Deforestation rates (0, 50, 80%)					
	Chi-square	*p*-value	Chi-square	*p*-value	0% vs. 50%	0% vs. 80%	50% / 0%	80% / 0%
Catchment								
Discharge	8.08	0.018*	13.89	0.001***	0.021*	0.001***	6.8%	10.2%
NO_3—N	3.31	0.191	432.80	0.000***	0.000***	0.000***	73.3%	113.8%
TP	0.75	0.686	343.40	0.000***	0.000***	0.000***	29.9%	56.0%
SRP	0.56	0.756	442.60	0.000***	0.000***	0.000***	39.5%	74.5%
PP	0.48	0.788	36.00	0.000***	0.004**	0.000***	11.5%	19.2%
Reservoir								
Water Temp.	13.32	0.001**	0.08	0.96	0.96	0.96	-[a]	-[a]
TN	2.59	0.274	396.91	0.000***	0.000***	0.000***	41.8%	65.4%
TP	0.16	0.923	444.51	0.000***	0.000***	0.000***	25.4%	40.8%
NO_3—N	3.48	0.175	390.65	0.000***	0.000***	0.000***	78.9%	122.1%
SRP	0.05	0.977	406.72	0.000***	0.000***	0.000***	68.7%	85.4%
PP	0.12	0.943	64.49	0.000***	0.002**	0.000***	14.7%	49.8%
Chl-a	1.46	0.483	364.27	0.000***	0.000***	0.000***	15.0%	30.7%
Cyanobacteria	3.46	0.178	383.89	0.000***	0.000***	0.000***	21.2%	36.2%
Green algae	1.77	0.412	291.82	0.000***	0.000***	0.000***	189.1%	228.0%
Diatom	2.98	0.226	204.24	0.000***	0.000***	0.000***	34.9%	80.0%
TSI	0.78	0.678	424.70	0.000***	0.000***	0.000***	5.6%	9.5%

90% of variance in annually-average discharge is not explained by either climate change or deforestation (Fig. 3f). In addition, no temporal change is found in discharge under any scenario projection (MK test, $p > 0.05$; Fig. S7).

For nutrient concentration in the Rappbode catchment, the model predicts that deforestation is the main driver of changes (KW test, $p < 0.001$) while climate has no significant direct effect (KW test, $p > 0.05$) (Fig. 3, Table 2). The increase of nutrient concentrations ranged 12% - 114% under both 50 and 80% deforestation compared to the reference scenario with no deforestation (Table 2). At 80% deforestation, nutrient concentrations in Rappbode catchment increase but remained significantly lower than those in Hassel under 0% deforestation, and discharge

will be significantly higher than that in Hassel (Wilcoxon test, $p < 0.001$; Fig. 3). Multilevel models further reveal that deforestation explained ca. 63%, 50% and 64% of the variations in NO_3—N, TP and SRP concentrations (Fig. 3f). Similar to discharge, PP is not well explained by either factor (>95% variance explained by residuals). For NO_3—N, there is a significant increasing trend only at RCP8.5 under different deforestations (MK test, $p < 0.01$; Fig. S7). For TP and SRP, a significant increasing trend is detected under each RCP and deforestation scenario (MK test, $p < 0.01$). For PP, no temporal trend is found in any scenario.

3.3. Reservoir model calibration and validation

For both reservoirs, simulated water temperature showed high accuracy with *RMSE* below 1.0 °C, *R* higher than 0.98 and *PBIAS* below 4% in both calibration and validation, respectively, (Figs. 4 and S8, Tables S4 and S5), indicating that the model well captured the thermal dynamics on the vertical dimension. In addition, the highly variable DO dynamics in the epilimnion and the deep-water hypoxia were both successfully modeled, with *R* ~0.9 and *PBIAS* below 30% in Rappbode, and *R* ~0.8 and *PBIAS* below 20% in Hassel.

The model succeeded in predicting the inter- and intra-annual variations in NO_3—N, with *R* of 0.55/0.68 and *PBIAS* of 15%/12% for calibration/validation, respectively, (Figs. 4, S9, S11 and S12). The model performed better during the second validation (2011–2019, only surface data), with *R* ~0.9 and *PBIAS* about 15% (Figs. S10 and S13, Tables S4 and S5). Summer depletion of NO_3—N was nicely captured by the model. Simulated NH_4—N also agreed reasonably with observations. The model underestimated the summer NH_4—N peaks during calibration. The model overall showed an acceptable performance for TN with *R* higher than 0.5.

The model succeeded in grasping the magnitude and variations of TP with *R* ~0.3 and *PBIAS* ~30% for both calibration and validation despite its low level (0.01–0.03 mg L^{-1}). Several TP peaks in both reservoirs were not captured by the model. Besides, the model captured the magnitude of SRP, which was occasionally above the detection limit (0.003 mg L^{-1}) in Rappbode predam during autumn-winter and remained mostly undetectable in other seasons. In addition, silicon concentration was captured in terms of both seasonal variations and inter-annual magnitude in both reservoirs, with *R* ~0.26/0.39 and *PBIAS* around 20% in calibration and validation, respectively, and better

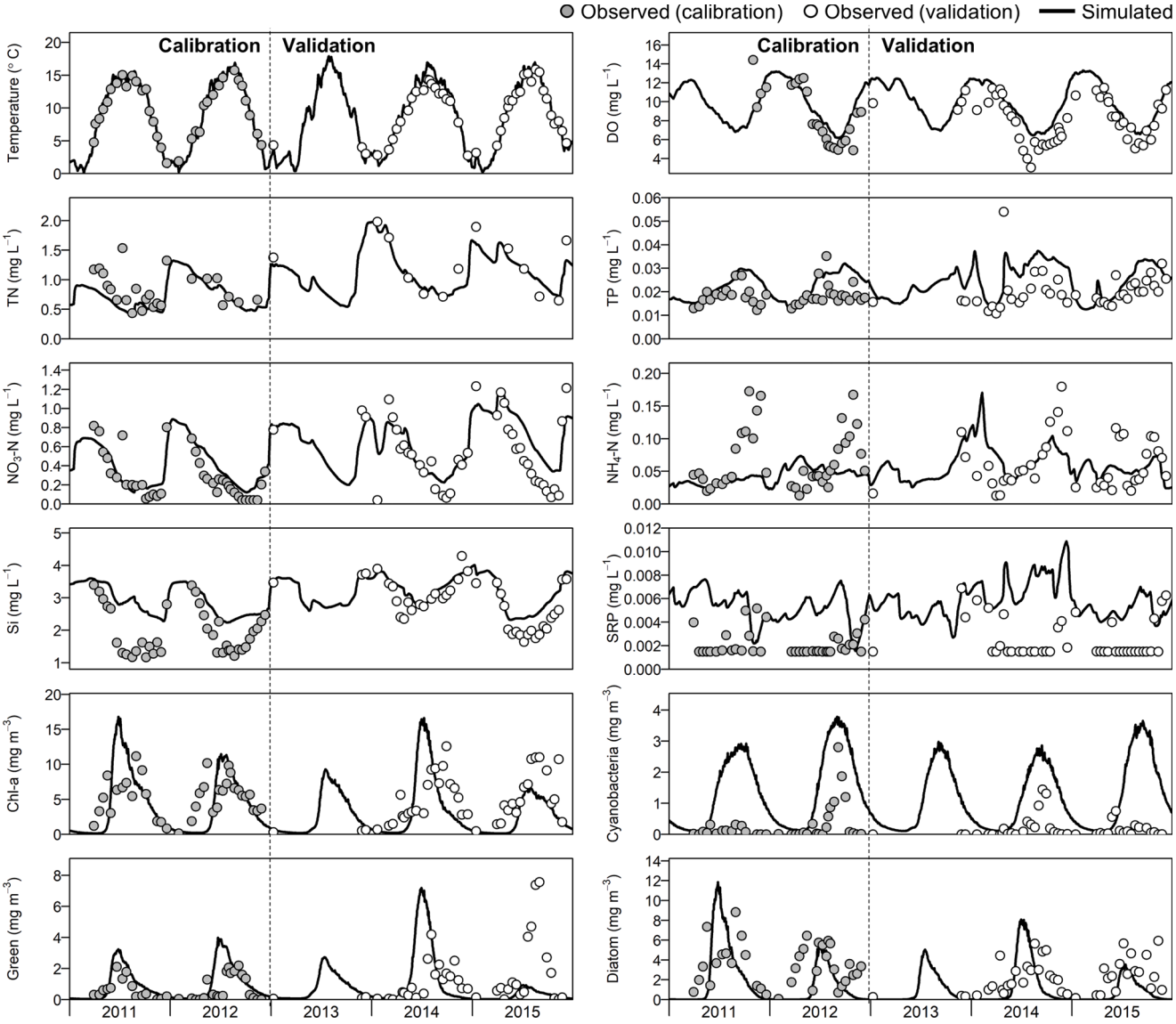

Fig. 4. Performance of the reservoir ecosystem model (GOTM-WET) in the Rappbode predam. Observed and simulated data were compared for water temperature and water quality variables from 2011 to 2015 for both calibration (2011–2012) and validation (2013–2015) periods. Volume-weighted values across the water column were provided. Note that the three algal groups (cyanobacteria, green algae and diatom) are provided as Chl-a concentration.

during second validation ($R > 0.8$) in Rappbode. In Hassel, *PBIAS* of simulated silicon was all below 8%.

The model predicted the magnitude and seasonality of Chl-a concentration reasonably well in both calibration and validation periods in both reservoirs, with *R* in the range 0.28–0.64 and *PBIAS* about 4–30%. The general patterns of phytoplankton community composition were nicely modeled, with *R* for cyanobacteria, green algae and diatom in the range 0.20–0.78 and *PBIAS* ranged 2.3–47.5%. The results showed that during 2011 to 2015, diatom and cyanobacteria were the dominant groups, while cyanobacteria was more abundant in Hassel than Rappbode (Figs. 4 and S11).

3.4. Projections of reservoir ecosystem dynamics

For TN, NO_3—N, TP, SRP and PP concentrations in Rappbode predam, model shows that differences among the deforestation gradients are significant but not among the climate change gradients (KW test; Fig. 5, Table 2). In specific, compared to 0% deforestation, 50 and 80% deforestation lead to a significant increase of nutrient concentration (TN, NO_3—N, TP, SRP and PP) ranged 14.7–122.1% (Table 2). At 80% deforestation, nutrient concentrations (except for PP) in Rappbode remain lower than those in Hassel at 0% deforestation (Wilcoxon test, $p < 0.05$). Nevertheless, TP and SRP concentrations both approach to the level in Hassel (Fig. 5). Multilevel model shows that deforestation accounts for 70–82% of variance in concentrations of TN, TP, NO_3—N and SRP, and 12% in PP (Fig. 5). Despite 14.7–49.8% increase in PP concentration at 50 and 80% deforestation, respectively, in-lake biogeochemical processes are more important than external inputs, resulting in the low explanatory of variance in PP. Climate change shows no direct contribution to the variations in nutrient concentrations. All nutrient concentrations (except for PP) show a significant increasing trend over the projection period (MK test, $p < 0.05$) (Fig. S14).

The model projections suggest that, for Chl-a concentration, three algal biomass and *TSI*, differences among the deforestation gradients are

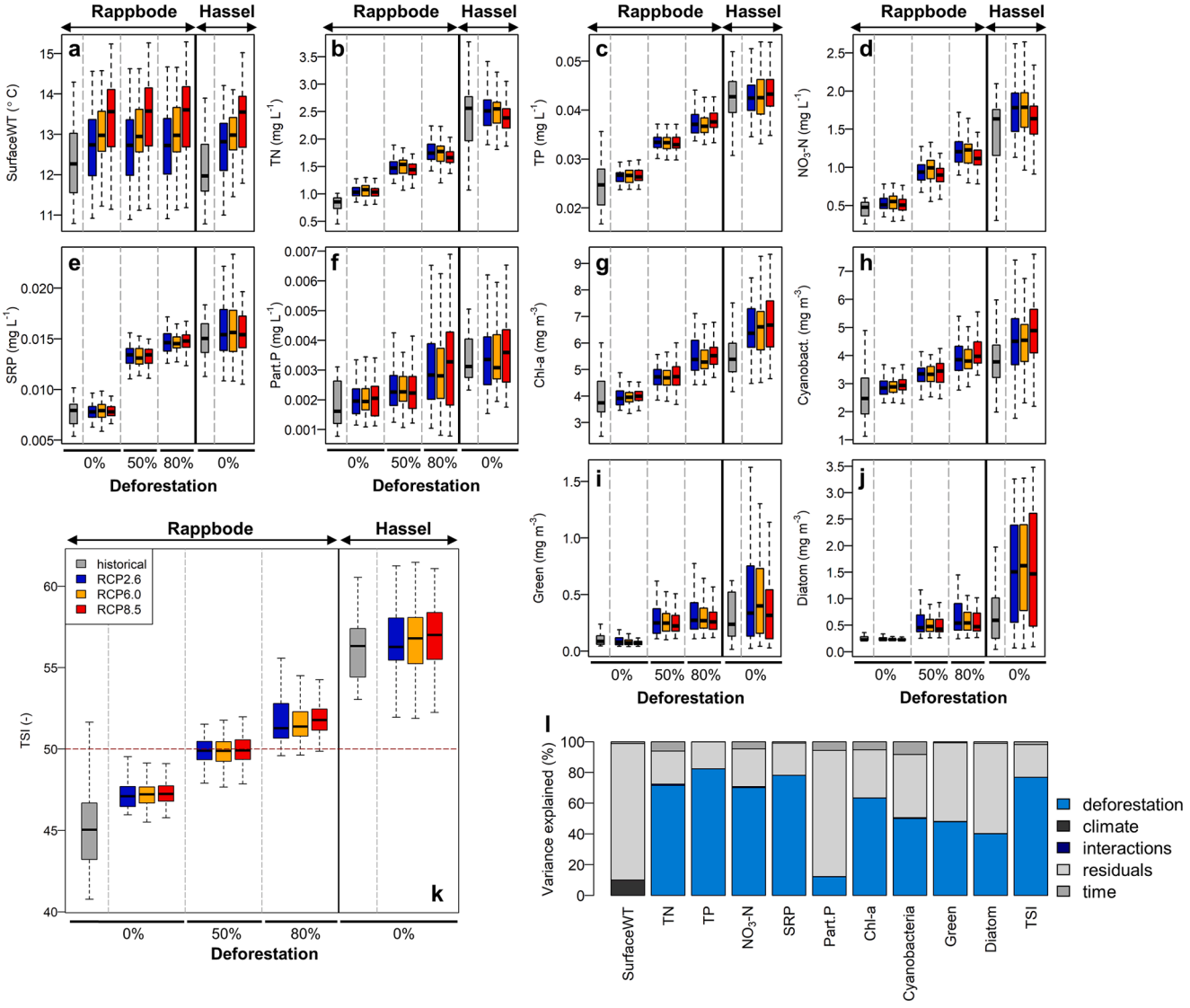

Fig. 5. Projections of reservoir ecosystem dynamics by GOTM-WET. (a-k) Projections for different water quality variables and trophic state index (*TSI*) in both Rappbode and Hassel predams at annually-averaged scale. 30<*TSI*<50: mesotrophic; *TSI*>50: eutrophic. The projections include the scenarios of four climate projections (historical and RCPs 2.6, 6.0 and 8.5) and three deforestation rates (0, 50 and 80%). 'Historical' scenario is the simulated data in the reservoirs from 2011 to 2018 before the deforestation, and the other scenarios are from 2021 to 2035. For Hassel, only 0% deforestation is projected serving as a reference state for eutrophic systems. See Fig. S14-S16 for the time series of these data at a daily scale. (l) Relative contributions of different factors in explaining the variance of various variables projected in the Rappbode predam, determined by multilevel analysis on the model projections. Note that 'interactions' denote the interactions between deforestation and climate change.

significant but not among the climate change gradients (KW test; Fig. 5, Table 2). In specific, at 50 and 80% deforestation, the model predicts an increase of Chl-a concentration and three algal biomass ranged 15–228% (Table 2), where green algae and diatom contribute a relative low proportion (7%−18%) of total algal biomass. Taken together, 50 and 80% deforestation result in an increase of 5.6% and 9.5% in *TSI*, respectively, which ultimately exceed critical threshold of eutrophication (>50), indicating the eutrophication in Rappbode predam due to deforestation. Chl-a and three algal groups in Rappbode at 80% deforestation are still lower than those in Hassel (Wilcoxon test, $p < 0.05$), whereas they all approach to a similar level (Fig. 5). Furthermore, multilevel model shows that deforestation explains less variance in phytoplankton variables (40–63%) compared to that for nutrients (Fig. 5). From 2021 to 2035, Chl-a and cyanobacteria both show a significant increase trend under all projection scenarios (MK test, $p < 0.05$; Fig. S15). In contrast, green algae and diatom show an increasing trend under RCP2.6 but decreasing trend under RCP6.0 and RCP8.5 (MK test, $p < 0.05$; Fig. S15). Finally, water temperature is only affected by climate change but not by deforestation, and no significant change was detected in water temperature, thermocline depth and Schmidt stability from 2021 to 2035 (Fig. S16). Overall, the model projects a shift to eutrophication state in the mesotrophic Rappbode predam at 80% deforestation. Phytoplankton biomass appears to respond to deforestation and climate change in a more diverse pattern than nutrients.

4. Discussion

4.1. Impact of deforestation on catchment dynamics

Our results on the impact of deforestation on discharge are in line with a few available long-term field observations in temperate areas. In the Rappbode catchment, no significantly increased discharge was observed under 17.1% deforestation in 2020 (Fig. S17, SI text). The extreme drought in 2018 was associated with lower precipitation, while the runoff:precipitation ratio only fluctuated without clear trends (Fig. S18). Beudert et al. (2018) pointed out that deforestation rate must exceed a threshold of 20–25% of the total catchment area to be detectable in discharge (with precipitation higher than 500 mm y^{-1}). However, discharge was found unchanged over 30 years after a 40% deforestation in 2005 in the Bavarian forest (Jung et al., 2021). In addition, our model projections suggest a slightly increased discharge by 6.8% and 10.2% under 50% and 80% deforestation, respectively (Fig. 3, Table 2). The low increase of discharge in response to deforestation can be explained by a mixture of competing factors of reduced evapotranspiration from grassland fallow compared to conifer forest (Fig. S19), and increased evaporation of grassland due to loss of the shading by the canopy and an increased evapotranspiration for all vegetation types due to global warming, which may reduce the differences in evapotranspiration between the vegetation types.

NO_3—N concentration is predicted to increase by 78.9% under 50% deforestation (Table 2), while it was found doubled in Bavarian forest after 40% deforestation (Jung et al., 2021). Similar extent of NO_3—N concentration increase after drastic deforestation was also reported in Hubbard Brook Experimental Forest (US) (Bormann et al., 1974) and Plešné national park (Kopáček et al., 2017). Our model suggests that the increase in NO_3—N concentration is mainly due to reduced NO_3—N uptake by tree vegetation and thereby lower N-storage in the catchment. In combination with lower transpiration, this leads to increased soil moisture and NO_3—N increasing leaching from the soil after deforestation. Compared to N, the increase in P after deforestation was less pronounced. The dominant change occurred in SRP and TP, whereas PP was only slightly affected. The projected increase of SRP in the Rappbode catchment under 80% deforestation (85.4%) is consistent with that in the Plešné national park, where SRP concentration in the streams increased by 50–100% after deforestation (Kopáček et al., 2017). Our model suggests that the lower P plant uptake in combination with slightly elevated soil moisture and related dissolution of P from soil increases soluble P availability. An increasing SRP availability due to higher water table and soil moisture can also be supported by associated changing redox conditions (Kopáček et al., 2017), which is not explicitly considered by our model. Intriguingly, suspended PP only slightly increased after deforestation because dense grassland vegetation sheltered the soil surface and prevents soil loss due to upland erosion, which was explicitly modeled by HYPE. Continuous monitoring data from the Rappbode catchment outlet partially confirm the consistent changing trends with model projections (see SI text; Fig. S17). Existing monitoring is proceeded to trace the change in the years to come.

4.2. Impact of deforestation on reservoirs

We provide concrete evidence of noteworthy potential of reservoirs water quality deterioration by deforestation. The projected eutrophication in the downstream reservoir (Rappbode) resulted in a higher production of algal biomass (Fig. 5), particularly at 80% deforestation scenario. Meanwhile, the influence of warming-induced lake physical changes (Huisman et al., 2018) acts as a secondary role in driving the phytoplankton development (Figs. S16 and S20). The magnitude of increase in cyanobacteria (21–36%) in response to deforestation is in line with a recent global projection until 2050 (20–30%), in which both climate and anthropogenically-driven land-use changes are found to be associated with algal biomass increase (Kakouei et al., 2021). Interestingly, cyanobacteria increased less than the other groups in relative terms (Fig. 5). Cyanobacteria can be generally regarded as more competitive under nutrient limitation (especially N limitation) than the other groups. Accordingly, although cyanobacteria increased the most in absolute terms due to higher nutrient levels, the degree of nutrient limitation decreased, and consequently so did the competitive advantage of cyanobacteria, allowing the diatoms and green algae to increase in biomass more in relative terms. This is evident in the strong correlation of nutrients with diatoms and green algae, but weaker correlation with cyanobacteria (Fig. S20). Nevertheless, the response of the algal composition to nutrient enrichment is difficult to generalize and likely occurs more at the species level (Kong et al., 2021; Shatwell et al., 2013) rather than in the broad taxonomic groups. Overall, together with the findings from catchment modeling showing a higher impact of deforestation than climate change (Fig. 3), our results emphasize the need to focus more on catchment land use changes (particularly by climate change) in the near future for downstream lakes/reservoirs water quality.

Intriguingly, variations in the phytoplankton projections are not as well explained by the climate and deforestation factors (40–63%) as those for the nutrient variables (70–82% excluding PP) (Fig. 5). Controlling factors beyond climate and deforestation, such as top-down effect of grazing and competition between macrophytes and phytoplankton, may also play a crucial role in mediating the phytoplankton development in future scenarios (Rousso et al., 2020). Hence, projections on phytoplankton can be accurately achieved when both external forcing and process-based models accounting for internal ecological descriptions in the lake/reservoir are available, which is exemplified in the present study.

We deem that the findings in the current study can be relevant for many other similar catchment-reservoir systems in temperate regions. Catchment-reservoir systems are widely distributed particularly in natural temperate forested areas (van Wijk et al., 2021). Due to an increasing frequency of droughts projected in the future (Hari et al., 2020), we envision an increasing deforestation risk, which may exert profound impacts on forest ecosystems and corresponding surface waters like rivers, lakes, and reservoirs by stimulating matter flux from the catchments. Our results, therefore, call for a more comprehensive evaluation of deforestation combining both catchment and ecosystem-level dynamics in the receiving stagnant waters.

4.3. Merits and limitations of the coupled modeling approach

Our model coupling benefits vastly from the recent development of both catchment and aquatic ecosystem process-based models (Janssen et al., 2019; Rode et al., 2010). Moreover, our modeling approach distinguished from the existing studies because we coupled catchment and reservoir models at a process-based level and validated the model across a period with rapid changes. Such model coupling requires a detailed configuration, calibration/validation, and projection procedures and harmonized teamwork in both compartments. Despite emerging tools such as QWET (Nielsen et al., 2021), insights from both catchment and lake expertises are eternally essential. In addition, our model was calibrated and validated against field observations of 10 years (2010–2019), covering a period with rapid change due to climate warming and deforestation (Figs. 2, S10 and S13). Therefore, our study showcases the capacity of process-based models in capturing ecosystems dynamics under changing external conditions, which enhances the reliability of the future projections.

In addition, we developed the coupled model in two adjacent reservoir systems with distinct ecological states. We propose that it is valuable to conduct an 'ensemble sites' approach, that is, to develop one process-based model with identical parameters to multiple similar catchment-lake systems to prove transferability of the underlying model system. The parameter set of the catchment model is applicable for both natural and agricultural-dominant catchments, while the parameter set of the reservoir model represents both meso-trophic and eutrophic states of reservoirs, covering a wide gradient of catchment-reservoir systems. For example, the two catchments largely differ in land use but both are well simulated for discharge using the same land use related parameters, which gives us strong confidence in the reliability of land use dependent evapotranspiration parameters. In addition, the model is able to reflect decisive ecosystem characteristics not only to the timing and magnitude of single variables but also to important key properties. The simulations showed a more eutrophic state for Hassel compared to Rappbode reflected by nutrient concentrations and phytoplankton biomass and composition. The shift from diatoms towards cyanobacteria with increasing phosphorus supply is a key feature along the eutrophication gradient. Such comparative studies turn out to be insightful with respect to identifying fundamental principles, e.g., by using reference states (Carpenter et al., 2011) or by comparing gradients of environmental drivers on ecological processes (Jeppesen et al., 2020). In conclusion, we suggest incorporating such a comparative limnological perspective more in the future modeling practice to improve trust in the model validity for projection.

Nevertheless, the current catchment modeling approach has limitations because the transient deforestation is missing and unlinked to climate change in the catchment modeling. The deforestation scenarios (50 and 80%) are currently modeled as a 'sudden' shift in the land use, whereas such a process is more progressive in reality. For example, NO_3—N concentration was found to increase immediately after deforestation or lagging one growing season, but generally peaks in 5–7 years after deforestation (Jung et al., 2021; Schmidt et al., 2021). Thus, we are modeling the 'worst case' scenario and cautions are needed when linking model projections to management practice. In addition, the deforestation scenarios are not causally linked to climate change. Further studies are expected to incorporate more terrestrial dynamics in the catchment modeling to capture the delay in stream nutrient level changes. Moreover, reforestation will take place after the deforestation, which again is a transient process and specific reforestation management options will lead to deviating forest developments and associated nutrient export to fluvial and stagnant waters. For future modeling approach, we recommend the coupling of a forest growth model (Bugmann et al., 2019) with the catchment nutrient export model. Lastly, deforestation may increase the sensitivity of discharge to extreme precipitation events at sub-daily scale. Unfortunately, due to the limitation in the spatial context of precipitation data and the daily time step of the model, extreme events could only be partly captured by HYPE. Thus, a few extreme nutrient peaks are not well captured within the calibration and validation period (Fig. 2), which opens the opportunity for further improvement based on increasing data availability and finer model resolution.

4.4. Implications for climate impact on reservoirs: a time-scale-dependent framework

Our analyses underscore the need for revisiting our current focus in understanding the external drivers of lake/reservoir ecosystems in a time-scale dependent framework. Recent studies highlight the pronounced direct impact of climate changes (till 2100) in temperature and mixing regime (Woolway and Merchant, 2019), lake oxygen (Jane et al., 2021) and thermal habitat (Kraemer et al., 2021). However, such changes require at least decades in the future to become detectable. Our study reveals that in a shorter time scale (i.e., 1-2 decades), changes in catchment land use such as deforestation will likely lead to eutrophication in the reservoirs, while the direct impacts of climate change remained limited. This is the key interpretation of our work and thus lays a foundation for a field of research related to climate change impact studies: indirect impacts from climate change are likely to be much more profound than the direct impacts in the next 1-2 decades. This state also points to extreme events, which have the potential to change whole ecosystems within a reasonable short time. In addition to deforestation, other processes may turn out to be of similar importance, e.g., loss of key species or invasion of new ones (Bell et al., 2021), groundwater drawdowns and accompanying habitat loss of aquatic ecosystems (Rinke et al., 2021).

Therefore, we advocate a timescale-dependent framework to tackle the climate change impact on the catchment-reservoir systems (Fig. 6), in which both short-term, indirect impacts and long-term direct impacts are summarized. Specifically, in the time scale of next 1-2 decades, indirect effects of climate change on lake/reservoirs via catchment changes would be dominant, calling for a focus on catchment and improved nutrient management practice. On a longer time scale (up to 2100), increasing direct impact from climate change are expected, particularly in the worst scenario (RCP8.5) (Woolway et al., 2020), in parallel with more severe changes in the catchments (e.g., deforestation). At this stage, both catchment management and climate adaptation strategies in downstream reservoirs such as selective-withdrawal strategy (Mi et al., 2020) and optimum water transport (Zhan et al., 2021), will be highly recommended.

5. Conclusions

- The present study demonstrates that deforestation in temperate natural catchments results in an increased nutrient loading and can ultimately turn downstream mesotrophic reservoirs into a eutrophic state.
- The enhanced nutrient loading (N and P) to the reservoirs after deforestation is attributed predominantly to the increasing nutrient concentration in the streams due to lower nutrient storage and uptake, higher nutrient concentration in soil water and raised soil nutrient leaching in the catchments, but marginally to the increasing discharge.
- Our results highlight the predominant indirect effect of climate change on lakes/reservoirs via changing land use and catchment nutrient loading in the next 10–20 years. Direct effects of climate change on lakes/reservoirs remain limited compared to indirect catchment effects in this short-term scale but may become increasingly significant in the long run due to enhanced profound changes in thermal dynamics.
- As a modeling approach, the present study exemplifies the joint strength of coupled catchment and lake/reservoir process-based model in elucidating the complex causality chain from climate

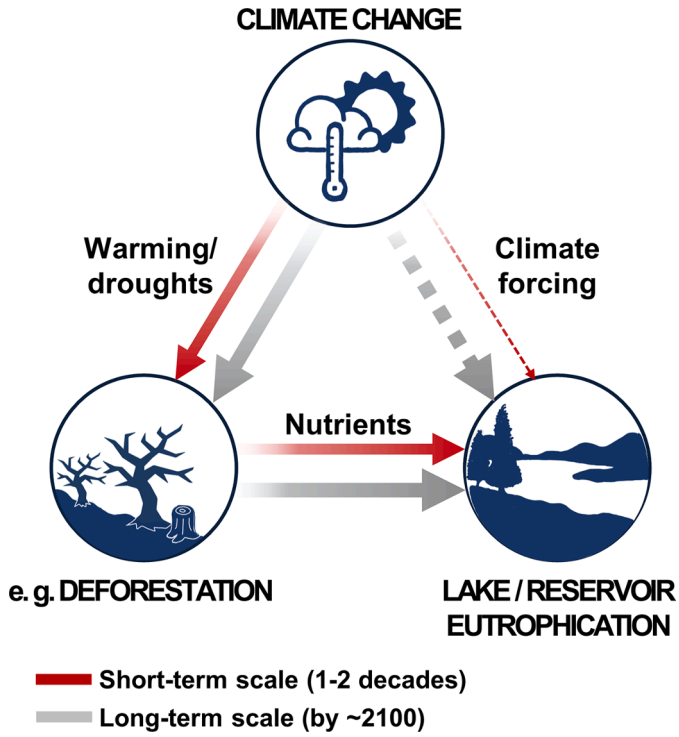

Fig. 6. A conceptual framework to elucidate the climate impact on the catchment-reservoir systems in both short- and long-term time scales. In the short-term scale (1–2 decades), indirect effects of climate change (solid arrows) as mediated by catchment dynamics, e.g., deforestation, will be more influential than the direct impacts of climate warming to the lakes/reservoirs, with vast potential of water quality deterioration and eutrophication. In the long-term scale (till 2100), however, direct impact of climate change (dashed arrows) on lake/reservoir water quality will be more pronounced, while the indirect effects are also envisioned to be enhanced in parallel, ultimately resulting in the equally importance of both impact pathways.

change to catchment-reservoir ecosystems. The unique dual system in this study site demonstrates the enormous value of comparative studies to improve the robustness of numerical model projections.

- Finally, we propose to evaluate the climate change impact on lakes/reservoirs under an updated framework with time-scale dependency, i.e., prioritizing the implementation of adaptation strategies in the upstream catchment in the near future, and in the reservoir in the long-term scales.

Notes

The field data supporting this paper are available from the Zenodo online repository: http://doi.org/10.5281/zenodo.6617108.

Declaration of Competing Interest

The authors declare that they have no known competing financial interests or personal relationships that could have appeared to influence the work reported in this paper.

Acknowledgments

We thank our colleagues at Helmholtz centre for Environmental Research (UFZ) for valuable discussions at the early stage of this study. We thank the technician for their efforts to maintain the monitoring and UFZ Analytics Department (GEWANA) for performing the chemical analysis. The monitoring equipments were funded by TERENO (www.tereno.net) financed by the German Federal Ministry of Education and Research (BMBF). We also thank the editor and two anonymous reviewers who provided constructive comments and suggestions to improve the manuscript. This study is additionally funded by Invent-Water ITN (Inventive forecasting tools for adapting water quality management to a new climate) through the European Union's Horizon 2020 research and innovation program under the Marie Skłodowska-Curie grant agreement No. 956623. X. Kong is additionally supported by the National Key Research and Development Program of China (2019YFA0607100) and the National Natural Science Foundation of China (42177062). M. Determann is funded by the PhD college DYNAMO from UFZ. C. Mi is supported by the National Natural Science Foundation of China (42107060).

Supplementary materials

Supplementary material associated with this article can be found, in the online version, at doi:10.1016/j.watres.2022.118721.

References

Adrian, R., O'Reilly, C.M., Zagarese, H., Baines, S.B., Hessen, D.O., Keller, W., Livingstone, D.M., Sommaruga, R., Straile, D., Van Donk, E., 2009. Lakes as sentinels of climate change. Limnol. Oceanogr. 54 (6), 2283–2297.

Andersen, T.K., Bolding, K., Nielsen, A., Bruggeman, J., Jeppesen, E., Trolle, D., 2021. How morphology shapes the parameter sensitivity of lake ecosystem models. Environ. Model. Softw. 136, 104945.

Andersen, T.K., Nielsen, A., Jeppesen, E., Hu, F., Bolding, K., Liu, Z., Søndergaard, M., Johansson, L.S., Trolle, D., 2020. Predicting ecosystem state changes in shallow lakes using an aquatic ecosystem model: lake Hinge, Denmark, an example. Ecol. Appl. 30 (7), e02160.

Barbosa, C.C., do Carmo Calijuri, M., Dos Santos, A.C.A., Ladwig, R., de Oliveira, L.F.A., Buarque, A.C.S, 2021. Future projections of water level and thermal regime changes of a multipurpose subtropical reservoir (Sao Paulo, Brazil). Sci. Total Environ. 770, 144741.

Bates, D., Mächler, M., Bolker, B. and Walker, S. 2014. Fitting linear mixed-effects models using lme4. arXiv:1406.5823.

Bell, D.A., Kovach, R.P., Muhlfeld, C.C., Al-Chokhachy, R., Cline, T.J., Whited, D.C., Schmetterling, D.A., Lukacs, P.M., Whiteley, A.R., 2021. Climate change and expanding invasive species drive widespread declines of native trout in the northern Rocky Mountains. USA Sci. Adv. 7 (52), eabj5471.

Bennett, N.D., Croke, B.F., Guariso, G., Guillaume, J.H., Hamilton, S.H., Jakeman, A.J., Marsili-Libelli, S., Newham, L.T., Norton, J.P., Perrin, C., 2013. Characterising performance of environmental models. Environ. Model. Softw. 40, 1–20.

Beudert, B., Bernsteinová, J., Premier, J., Bässler, C., 2018. Natural disturbance by bark beetle offsets climate change effects on streamflow in headwater catchments of the Bohemian Forest. Silva Gabreta 24, 21–45.

Beutler, M., Wiltshire, K.H., Meyer, B., Moldaenke, C., Lüring, C., Meyerhöfer, M., Hansen, U.P., Dau, H., 2002. A fluorometric method for the differentiation of algal populations *in vivo* and *in situ*. Photosynth. Res. 72 (1), 39–53.

Boczoń, A., Kowalska, A., Ksepko, M., Sokołowski, K., 2018. Climate warming and drought in the Bialowieza Forest from 1950 to 2015 and their impact on the dieback of Norway Spruce stands. Water 10 (11), 1502 (Basel).

Boessenkool, B. 2019. rdwd: select and download climate data from 'DWD' (German weather service). R package version 1.2.0. https://CRAN.R-project.org/package=rdwd.

Bolding, K. and Bruggeman, J. 2020 Parsac: parallel sensitivity analysis and calibration.

Bormann, F.H., Likens, G., Siccama, T., Pierce, R., Eaton, J., 1974. The export of nutrients and recovery of stable conditions following deforestation at Hubbard Brook. Ecol. Monogr. 44 (3), 255–277.

Bugmann, H., Seidl, R., Hartig, F., Bohn, F., Brůna, J., Cailleret, M., François, L., Heinke, J., Henrot, A.J., Hickler, T., 2019. Tree mortality submodels drive simulated long-term forest dynamics: assessing 15 models from the stand to global scale. Ecosphere 10 (2), e02616.

Carlson, R.E., 1977. A trophic state index for lakes. Limnol. Oceanogr. 22 (2), 361–369.

Carpenter, S.R., Cole, J.J., Pace, M.L., Batt, R., Brock, W.A., Cline, T., Coloso, J., Hodgson, J.R., Kitchell, J.F., Seekell, D.A., Smith, L., Weidel, B., 2011. Early warnings of regime shifts: a whole-ecosystem experiment. Science 332 (6033), 1079–1082.

Couture, R.M., Tominaga, K., Starrfelt, J., Moe, S.J., Kaste, Ø., Wright, R.F., 2014. Modelling phosphorus loading and algal blooms in a Nordic agricultural catchment-lake system under changing land-use and climate. Environ. Sci.: Process. Impacts 16 (7), 1588–1599.

Déqué, M., Rowell, D., Lüthi, D., Giorgi, F., Christensen, J., Rockel, B., Jacob, D., Kjellström, E., De Castro, M., van den Hurk, B., 2007. An intercomparison of regional climate simulations for Europe: assessing uncertainties in model projections. Clim. Change 81 (1), 53–70.

Domis, L.N.D., Elser, J.J., Gsell, A.S., Huszar, V.L.M., Ibelings, B.W., Jeppesen, E., Kosten, S., Mooij, W.M., Roland, F., Sommer, U., Van Donk, E., Winder, M., Lurling, M., 2013. Plankton dynamics under different climatic conditions in space and time. Freshwat. Biol. 58 (3), 463–482.

Downing, J., McClain, M., Twilley, R., Melack, J., Elser, J., Rabalais, N.N., Lewis, W., Turner, R.E., Corredor, J., Soto, D., 1999. The impact of accelerating land-use change on the N-cycle of tropical aquatic ecosystems: current conditions and projected changes. Biogeochemistry 46 (1), 109–148.
Friese, K., Schultze, M., Boehrer, B., Buttner, O., Herzsprung, P., Koschorreck, M., Kuehn, B., Ronicke, H., Tittel, J., Wendt-Potthoff, K., Wollschlager, U., Dietze, M., Rinke, K., 2014. Ecological response of two hydro-morphological similar pre-dams to contrasting land-use in the Rappbode reservoir system (Germany). Int. Rev. Hydrobiol. 99 (5), 335–349.
Ghaffar, S., Jomaa, S., Meon, G., Rode, M., 2021. Spatial validation of a semi-distributed hydrological nutrient transport model. J. Hydrol. 593, 125818.
Hari, V., Rakovec, O., Markonis, Y., Hanel, M., Kumar, R., 2020. Increased future occurrences of the exceptional 2018–2019 Central European drought under global warming. Sci. Rep. 10 (1), 1–10.
Harrison, J.A., Maranger, R.J., Alexander, R.B., Giblin, A.E., Jacinthe, P.A., Mayorga, E., Seitzinger, S.P., Sobota, D.J., Wollheim, W.M., 2009. The regional and global significance of nitrogen removal in lakes and reservoirs. Biogeochemistry 93 (1–2), 143–157.
Hoffman, G.E., Schadt, E.E., 2016. variancePartition: interpreting drivers of variation in complex gene expression studies. BMC Bioinform. 17 (1), 1–13.
Hu, F., Bolding, K., Bruggeman, J., Jeppesen, E., Flindt, M., van Gerven, L., Janse, J., Janssen, A., Kuiper, J., Mooij, W., 2016. FABM-1 PCLake-linking aquatic ecology with hydrodynamics. Geosci. Model Dev. 9 (2), 2271–2278.
Huisman, J., Codd, G.A., Paerl, H.W., Ibelings, B.W., Verspagen, J.M., Visser, P.M., 2018. Cyanobacterial blooms. Nat. Rev. Microbiol. 16 (8), 471–483.
Jane, S.F., Hansen, G.J., Kraemer, B.M., Leavitt, P.R., Mincer, J.L., North, R.L., Pilla, R. M., Stetler, J.T., Williamson, C.E., Woolway, R.I., 2021. Widespread deoxygenation of temperate lakes. Nature 594 (7861), 66–70.
Janse, J.H., 2005. Model Studies On the Eutrophication of Shallow Lakes and Ditches. Wageningen University, Wageningen, The Netherlands [Doctoral Dissertation].
Janse, J.H., Scheffer, M., Lijklema, L., Van Liere, L., Sloot, J.S., Mooij, W.M., 2010. Estimating the critical phosphorus loading of shallow lakes with the ecosystem model PCLake: sensitivity, calibration and uncertainty. Ecol. Model. 221 (4), 654–665.
Janssen, A.B., Janse, J.H., Beusen, A.H., Chang, M., Harrison, J.A., Huttunen, I., Kong, X., Rost, J., Teurlincx, S., Troost, T.A., van Wijk, D., Mooij, W.M., 2019. How to model algal blooms in any lake on earth. Curr. Opin. Environ. Sustain. 36, 1–10.
Jeppesen, E., Canfield, D.E., Bachmann, R.W., Søndergaard, M., Havens, K.E., Johansson, L.S., Lauridsen, T.L., Sh, T., Rutter, R.P., Warren, G., 2020. Toward predicting climate change effects on lakes: a comparison of 1656 shallow lakes from Florida and Denmark reveals substantial differences in nutrient dynamics, metabolism, trophic structure, and top-down control. Inland Waters 10 (2), 197–211.
Jung, H., Senf, C., Beudert, B., Krueger, T., 2021. Bayesian hierarchical modeling of nitrate concentration in a forest stream affected by large-scale forest dieback. Water Resour. Res. 57 (2), e2020WR027264.
Kakouei, K., Kraemer, B.M., Anneville, O., Carvalho, L., Feuchtmayr, H., Graham, J.L., Higgins, S., Pomati, F., Rudstam, L.G., Stockwell, J.D., 2021. Phytoplankton and cyanobacteria abundances in mid-21st century lakes depend strongly on future land use and climate projections. Glob. Change Biol. 27 (24), 6409–6422.
Kong, X., Seewald, M., Dadi, T., Friese, K., Mi, C., Boehrer, B., Schultze, M., Rinke, K., Shatwell, T., 2021. Unravelling winter diatom blooms in temperate lakes using high frequency data and ecological modeling. Water Res. 190, 116681.
Kopáček, J., Fluksová, H., Hejzlar, J., Kaňa, J., Porcal, P., Turek, J., 2017. Changes in surface water chemistry caused by natural forest dieback in an unmanaged mountain catchment. Sci. Total Environ. 584, 971–981.
Kopáček, J., Kaňa, J., Porcal, P., Vrba, J., Norton, S.A., 2019. Effects of tree dieback on lake water acidity in the unmanaged catchment of Plešné Lake, Czech Republic. Limnol. Oceanogr. 64 (4), 1614–1626.
Kraemer, B.M., Pilla, R.M., Woolway, R.I., Anneville, O., Ban, S., Colom-Montero, W., Devlin, S.P., Dokulil, M.T., Gaiser, E.E., Hambright, K.D., 2021. Climate change drives widespread shifts in lake thermal habitat. Nat. Clim. Change 11 (6), 521–529.
Lawrence, D., Vandecar, K., 2015. Effects of tropical deforestation on climate and agriculture. Nat. Clim. Change 5 (1), 27–36.
Lindström, G., Pers, C., Rosberg, J., Strömqvist, J., Arheimer, B., 2010. Development and testing of the HYPE (Hydrological predictions for the environment) water quality model for different spatial scales. Hydrol. Res. 41 (3–4), 295–319.
McLeod, A.I., 2005. Kendall Rank Correlation and Mann-Kendall trend Test. R Package Kendall.
Mi, C., Shatwell, T., Ma, J., Xu, Y., Su, F., Rinke, K., 2020. Ensemble warming projections in Germany's largest drinking water reservoir and potential adaptation strategies. Sci. Total Environ. 748, 141366.
Mori, A.S., Lertzman, K.P., Gustafsson, L., 2017. Biodiversity and ecosystem services in forest ecosystems: a research agenda for applied forest ecology. J. Appl. Ecol. 54 (1), 12–27.
Mottl, O., Flantua, S.G., Bhatta, K.P., Felde, V.A., Giesecke, T., Goring, S., Grimm, E.C., Haberle, S., Hooghiemstra, H., Ivory, S., 2021. Global acceleration in rates of vegetation change over the past 18,000 years. Science 372 (6544), 860–864.
Nielsen, A., Hu, F.R.S., Schnedler-Meyer, N.A., Bolding, K., Andersen, T.K., Trolle, D., 2021. Introducing QWET–A QGIS-plugin for application, evaluation and experimentation with the WET model: environmental Modelling and Software. Environ. Model. Software 135, 104886.
Nielsen, A., Trolle, D., Bjerring, R., Søndergaard, M., Olesen, J.E., Janse, J.H., Mooij, W. M., Jeppesen, E., 2014. Effects of climate and nutrient load on the water quality of shallow lakes assessed through ensemble runs by PCLake. Ecol. Appl. 24 (8), 1926–1944.
Overpeck, J.T., Breshears, D.D., 2021. The growing challenge of vegetation change. Science 372 (6544), 786–787.
Pers, C., Temnerud, J., Lindström, G., 2016. Modelling water, nutrients, and organic carbon in forested catchments: a HYPE application. Hydrol. Process. 30 (18), 3252–3273.
R Core Team 2021 R: a language and environment for statistical computing. R foundation for statistical computing, Austria, URL http://www.R-project.org.
Rinke, K., Kuehn, B., Bocaniov, S., Wendt-Potthoff, K., Buttner, O., Tittel, J., Schultze, M., Herzsprung, P., Ronicke, H., Rink, K., Rinke, K., Dietze, M., Matthes, M., Paul, L., Friese, K., 2013. Reservoirs as sentinels of catchments: the rappbode reservoir observatory (Harz mountains, Germany). Environ. Earth Sci. 69 (2), 523–536.
Rinke, K., Mietz, S., Schneppmüller, M., 2021. Auswirkungen der dürreverhältnisse 2018-2020 auf die grundwasserstände in mitteldeutschland. Wasserwirtschaft 11, 49–56.
Rode, M., Arhonditsis, G., Balin, D., Kebede, T., Krysanova, V., Van Griensven, A., Van der Zee, S.E., 2010. New challenges in integrated water quality modelling. Hydrol. Process. 24 (24), 3447–3461.
Rode, M., Wade, A.J., Cohen, M.J., Hensley, R.T., Bowes, M.J., Kirchner, J.W., Arhonditsis, G.B., Jordan, P., Kronvang, B., Halliday, S.J., 2016. Sensors in the stream: the high-frequency wave of the present. Environ. Sci. Technol. 50 (19), 10297–10307.
Rousso, B.Z., Bertone, E., Stewart, R., Hamilton, D.P., 2020. A systematic literature review of forecasting and predictive models for cyanobacteria blooms in freshwater lakes. Water Res., 115959
Schmidt, S.I., Hejzlar, J., Kopáček, J., Paule-Mercado, M.C., Porcal, P., Vystavna, Y., 2021. Relationships between a catchment-scale forest disturbance index, time delays, and chemical properties of surface water. Ecol. Indic. 125, 107558.
Schnedler-Meyer, N.A., Andersen, T.K., Hu, F.R.S., Bolding, K., Nielsen, A., Trolle, D., 2022. Water ecosystems tool (WET) 1.0 – a new generation of flexible aquatic ecosystem model. Geosci. Model Dev. 2022 (15), 3861–3878.
Shatwell, T., Kohler, J., Nicklisch, A., 2013. Temperature and photoperiod interactions with silicon-limited growth and competition of two diatoms. J. Plankton Res. 35 (5), 957–971.
Storn, R., Price, K., 1997. Differential evolution–a simple and efficient heuristic for global optimization over continuous spaces. J. Glob. Optim. 11 (4), 341–359.
Sweeney, B.W., Bott, T.L., Jackson, J.K., Kaplan, L.A., Newbold, J.D., Standley, L.J., Hession, W.C., Horwitz, R.J., 2004. Riparian deforestation, stream narrowing, and loss of stream ecosystem services. Proc. Natl. Acad. Sci. USA 101 (39), 14132–14137.
Ullrich, A., Volk, M., 2010. Influence of different nitrate–N monitoring strategies on load estimation as a base for model calibration and evaluation. Environ. Monit. Assess. 171 (1), 513–527.
van Wijk, D., Teurlincx, S., Brederveld, R.J., de Klein, J.J., Janssen, A.B., Kramer, L., van Gerven, L.P., Kroeze, C., Mooij, W.M., 2021. Smart nutrient retention networks: a novel approach for nutrient conservation through water quality management. Inland Waters. https://doi.org/10.1080/20442041.20442020.21870852.
Vrugt, J.A., Robinson, B.A., Hyman, J.M., 2008. Self-adaptive multimethod search for global optimization in real-parameter spaces. IEEE Trans. Evol. Comput. 13 (2), 243–259.
Warszawski, L., Frieler, K., Huber, V., Piontek, F., Serdeczny, O., Schewe, J., 2014. The inter-sectoral impact model intercomparison project (ISI–MIP): project framework. Proc. Natl. Acad. Sci. USA 111 (9), 3228–3232.
Woodward, C., Shulmeister, J., Larsen, J., Jacobsen, G., Zawadzki, A., 2014. The hydrological legacy of deforestation on global wetlands. Science 346 (6211), 844–847.
Woolway, R.I., Kraemer, B.M., Lenters, J.D., Merchant, C.J., O'Reilly, C.M., Sharma, S, 2020. Global lake responses to climate change. Nat. Rev. Earth Environ. 1 (8), 388–403.
Woolway, R.I., Merchant, C.J., 2019. Worldwide alteration of lake mixing regimes in response to climate change. Nat. Geosci. 12 (4), 271–276.
Zemp, D., Schleussner, C.F., Barbosa, H., Rammig, A., 2017. Deforestation effects on Amazon forest resilience. Geophys. Res. Lett. 44 (12), 6182–6190.
Zhan, Q., Kong, X., Rinke, K., 2021. High-frequency monitoring enables operational opportunities to reduce the dissolved organic carbon (DOC) load in Germany's largest drinking water reservoir. Inland Waters. https://doi.org/10.1080/20442041.20442021.21987796.